

Chapter 4

Soil Reinforcing Mechanisms and Models

4.1 Introduction

In Chap. 3, you have learnt that when the fibres are included within a soil mass, they cause changes in the properties (e.g. permeability, compressibility, shear strength, etc.) of soil. The presence of fibres in a soil mass improves its stability, increases its load-carrying capacity and reduces its deformation (i.e. settlement and lateral movement). The effect of fibre inclusions on strength and stiffness behaviours of soil is explained through the role of fibres as a reinforcement element. This chapter presents the basic mechanisms and models of soil reinforcement, focusing on the random distribution of fibres within the soil mass, resulting in *randomly distributed fibre-reinforced soil* (RDFRS), or simply the *fibre-reinforced soil* (FRS), as explained in the previous chapters.

4.2 Basic Soil Reinforcing Mechanisms

If the reinforced soil is considered a homogeneous material, but with anisotropic characteristics, the Mohr-Coulomb failure criterion can be applied to explain the basic mechanism of reinforced soil. Consider a simplified situation, shown in Figs. 4.1a, b, where two cylindrical specimens of a cohesionless soil are subjected to the same triaxial loading with the minor principal stress (confining stress) σ_3 and the major principal stress σ_1 . The first soil specimen is not reinforced, but the second one is reinforced with fibres. Figure 4.1c shows a magnified view of the reinforced soil element, as indicated in Fig. 4.1b, with a horizontal fibre. Because of skin friction and/or adhesion between the fibre and the soil, the fibre applies a confining stress $\sigma_R (= \Delta\sigma_3, \text{ increase in the minor principal stress})$ on the soil, and in this process, the fibre gets stretched with mobilization of a tensile force T_f as shown

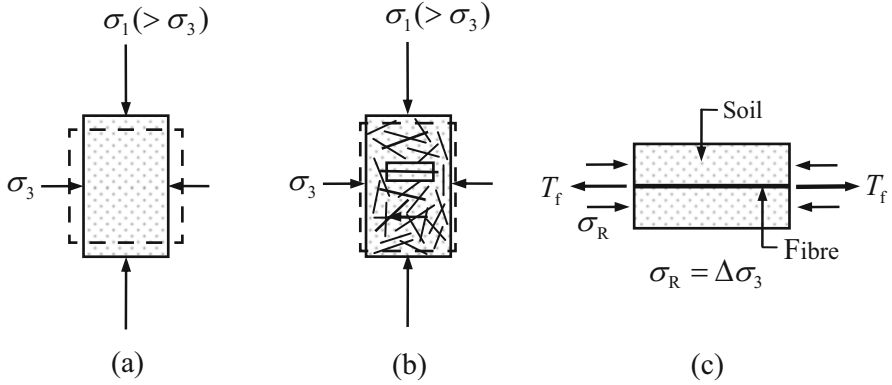


Fig. 4.1 Basic soil reinforcing mechanism: (a) unreinforced cylindrical soil specimen; (b) fibre-reinforced cylindrical soil specimen; (c) magnified view of a reinforced soil element, as indicated in (b)

in Fig. 4.1c. Note that the tensile force T_f and hence the confining stress σ_R will vary with orientation of the fibre within the soil mass.

Assume that the Mohr-Coulomb failure criterion has been attained in the unreinforced soil specimen. For this case, the stress state within the soil mass can be represented, in the normal stress (σ) and shear stress (τ) space, by a Mohr circle 'a' as shown in Fig. 4.2, which is tangent to the Mohr-Coulomb failure envelope l_U for the unreinforced soil. If the reinforced soil specimen is subjected to the same stress state, then due to skin friction and/or adhesion bonding between both constituents, the lateral deformation/strain of the specimen reduces. The lateral deformation of the reinforced soil specimen is generally greater than that of the reinforcement but smaller than the lateral deformation of the unreinforced soil specimen. This means that in the case of perfect friction and/or adhesion bonding between reinforcement and soil, the reinforcement is extended, resulting in a mobilized tensile force T_f , and the soil is compressed by additional compressive lateral stress as the reinforcement restraint $\sigma_R (= \Delta\sigma_3)$, introduced into the soil mass in the direction of the reinforcement as shown in Fig. 4.1c. The stress state in soil represented by the Mohr circle 'b' in Fig. 4.2 is no more tangent to the failure envelope l_U , and hence the reinforced soil specimen is able to sustain greater stresses than those in the case of unreinforced soil.

Consider that the reinforced soil specimen, shown in Fig. 4.1b, is expanding horizontally due to a decrease in applied horizontal stress σ_3 with a constant vertical stress σ_1 , and assume that the failure occurs by rupture of the reinforcement, that is, the lateral restraint σ_R is limited to a maximum value σ_{RCmax} depending on the strength of the reinforcement. This state of stress is represented by the Mohr circle 'c' in Fig. 4.2. The strength increase can be characterized by a constant cohesion intercept c_R as an apparent cohesion, introduced due to reinforcement (Schlosser and Vidal 1969). The results obtained from both the triaxial compression tests and the direct shear tests on sand specimens reinforced with tensile inclusions have

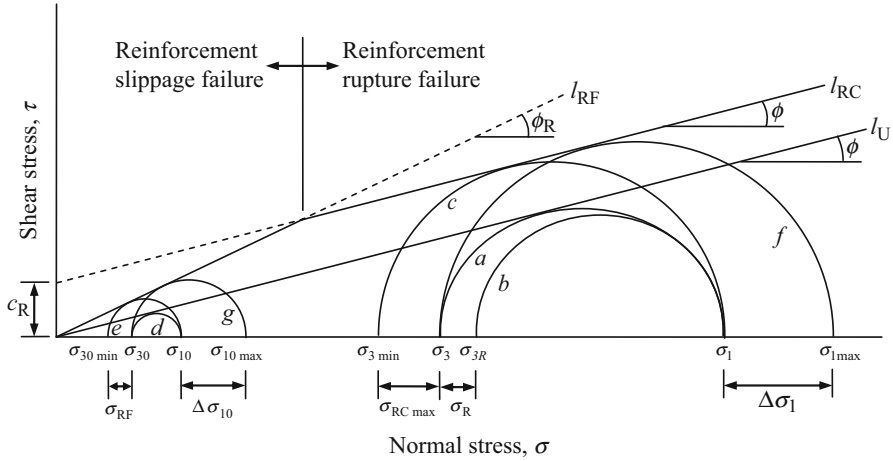


Fig. 4.2 Basic mechanism of fibre-reinforced soil: Mohr circles for reinforced and unreinforced cases

shown that the apparent cohesion of the reinforced soil is a function of the orientation of the inclusions with respect to the direction of the maximum extension in the soil (Long et al. 1972; Schlosser and Long 1974; Jewell 1980; Gray and Al-Refeai 1986). Thus, the strength envelope for a reinforced cohesionless soil for reinforcement rupture condition can be interpreted in terms of the Mohr-Coulomb failure envelope l_{RC} for the homogeneous cohesive soil as shown in Fig. 4.2.

For Mohr circle ‘a’, the principal stresses σ_1 and σ_3 are related as

$$\sigma_1 = \sigma_3 \tan^2(45^\circ + \phi/2) \tag{4.1}$$

where ϕ is the angle of shearing resistance (or angle of internal friction) of the unreinforced soil.

For Mohr circle ‘c’, representing the stress state of the reinforced soil at failure, the principal stresses σ_1 and σ_{3min} are related as

$$\sigma_1 = \sigma_{3min} \tan^2(45^\circ + \phi/2) + 2c_R \tan(45^\circ + \phi/2) \tag{4.2}$$

Since $\sigma_{3min} = \sigma_3 - \sigma_{RCmax}$, as seen in Fig. 4.2, Eq. (4.2) becomes

$$\sigma_1 = (\sigma_3 - \sigma_{RCmax}) \tan^2(45^\circ + \phi/2) + 2c_R \tan(45^\circ + \phi/2) \tag{4.3}$$

Combining Eqs. (4.1) and (4.3) leads to

$$c_R = \frac{\sigma_{RCmax} \tan(45^\circ + \phi/2)}{2} = \frac{\sigma_{RCmax} \sqrt{K_p}}{2} = \frac{\sigma_{RCmax}}{2\sqrt{K_a}} \tag{4.4}$$

where

$$K_a = \tan^2(45^\circ - \phi/2) \quad (4.5)$$

and

$$K_p = \tan^2(45^\circ + \phi/2) \quad (4.6)$$

Note that K_a and K_p are the Rankine's coefficients of active and passive lateral earth pressures, respectively. Also note that the anisotropic cohesion is produced in the direction of reinforcement orientation, and this concept is based on the laboratory shear strength studies on reinforced soil specimens.

You may now consider that the reinforced soil specimen shown in Fig. 4.1b is expanding horizontally due to a decrease in applied horizontal stress $\sigma_3 = \sigma_{30}$ with a constant vertical stress $\sigma_1 = \sigma_{10}$, as represented by the Mohr circle 'd', and assume that the failure occurs by a slippage between the reinforcement and the soil, that is, the lateral restraint σ_R is limited to σ_{RF} , which is proportional to σ_{10} . Therefore,

$$\sigma_{RF} = \sigma_{10}F \quad (4.7)$$

where F is a friction factor that depends on the cohesionless soil-reinforcement interface characteristics. This concept is based on the Yang's experimental results (Yang 1972) as presented by Hausmann and Vagneron (1977). The failure state of stress is represented by the Mohr circle 'e' in Fig. 4.2. The strength increase can be characterized by an increased friction angle ϕ_R . Thus, the strength envelope for a reinforced cohesionless soil for the reinforcement slippage condition can be interpreted in terms of the Mohr-Coulomb failure envelope l_{RF} for the homogeneous cohesionless soil as shown in Fig. 4.2.

For Mohr circle 'd', the principal stresses σ_{10} and σ_{30} are related as

$$\sigma_{10} = \sigma_{30} \tan^2(45^\circ + \phi/2) \quad (4.8)$$

Substituting Eq. (4.5) into Eq. (4.8) yields

$$\sigma_{10} = \frac{\sigma_{30}}{K_a} \quad (4.9)$$

For Mohr circle 'e', the principal stresses σ_{10} and $\sigma_{30\min}$ are related as

$$\sigma_{10} = \sigma_{30\min} \tan^2(45^\circ + \phi_R/2) \quad (4.10)$$

Since $\sigma_{30\min} = \sigma_{30} - \sigma_{RF}$, as seen in Fig. 4.2, Eq. (4.10) becomes

$$\sigma_{10} = (\sigma_{30} - \sigma_{RF}) \tan^2(45^\circ + \phi_R/2) \quad (4.11)$$

Substituting Eq. (4.7) into Eq. (4.11) yields

$$\sigma_{10} = (\sigma_{30} - \sigma_{10}F)\tan^2(45^\circ + \phi_R/2) \quad (4.12)$$

Combining Eqs. (3.8) and (3.12) leads to

$$1 = (K_a - F) \left(\frac{1 + \sin \phi_R}{1 - \sin \phi_R} \right)$$

or

$$\sin \phi_R = \frac{1 + F - K_a}{1 - F + K_a} \quad (4.13)$$

You may now consider that the reinforced soil specimen shown in Fig. 4.1b is expanding horizontally due to an increase in applied σ_1 with a constant σ_3 , and assume that the failure occurs by rupture of the reinforcement or reinforcement slippage. These failure states of stress are represented by the Mohr circles 'f' and 'g' in Fig. 4.2, respectively. Note that the reinforcement increases the compressive strength of the soil by $\Delta\sigma_1$ or $\Delta\sigma_{10}$ depending on the type of failure mode of the reinforced soil as indicated in the figure.

A different concept of the influence of reinforcement on the behaviour of reinforced soil mass was described by Basset and Last (1978). It is suggested that an introduction of reinforcement modifies the dilatancy characteristics of soil with a possible rotation of principal strain directions. This concept is based on the fact that if the dilation of the soil is restricted, the shear strength mobilized will be higher than for the case of no restriction. The presence of reinforcement in soil imposes a condition of restricted dilatancy. It also predetermines the principal incremental strain directions and rotates them relative to the unreinforced case, thereby resulting in a redistribution of stresses.

Note that the behaviour of soil reinforced with extensible reinforcements, such as geosynthetic reinforcements, does not fall entirely within the concepts as described here. For the details of reinforcing mechanisms of geosynthetic-reinforced soils, the readers may refer to the books by Shukla (2002, 2012, 2016) and Shukla and Yin (2006).

Example 4.1

For a reinforced sand, consider the following:

Angle of shearing resistance of unreinforced sand, $\phi = 33^\circ$

Friction factor, $F = 0.1$

Determine the angle of shearing resistance of the reinforced sand.

Solution

From Eq. (4.5), the Rankine's active earth pressure coefficient,

$$K_a = \tan^2(45^\circ - \phi/2) = \tan^2(45^\circ - 33^\circ/2) = 0.295$$

From Eq. (4.13),

$$\sin \phi_R = \frac{1 + F - K_a}{1 - F + K_a} = \frac{1 + 0.1 - 0.295}{1 - 0.1 + 0.295} = 0.674$$

Therefore, angle of shearing resistance of the reinforced sand is

$$\phi_R = \sin^{-1}(0.674) = 42.4^\circ$$

4.3 Basic Models of Fibre-Reinforced Soils

Based on the experimental studies, it has been established that the strength and deformation characteristics of the fibre-reinforced soils are governed by the soil and fibre characteristics as well as by confinement and stress level. The states of stress and strain in fibre-reinforced soils during its deformation and failure are complex. However, for engineering applications, it is possible to explain the mechanism of fibre reinforcements in soils, especially the contribution of fibres to the shear strength increase, and hence the behaviour of fibre-reinforced soils, by mathematical approaches/models. The finite element analyses considering appropriate constitutive relationships can be carried out to investigate the behaviour of fibre-reinforced soils. The commercial software can be used for such analyses without developing the complete codes. In the past, the researchers have attempted to present some simplified models, which are based on different approaches, such as force-equilibrium/mechanistic approach, energy dissipation approach, statistical approach and the approach of superposition of the effects of soil and fibres. Some of these models are presented here.

4.3.1 Waldron Model

The root-reinforced soil mass can be considered a composite material in which the roots of relatively a high tensile strength are embedded in a matrix of lower tensile strength. Waldron (1977) proposed a simple force-equilibrium model to estimate the increase in strength of soil reinforced with non-rigid plant roots, taking into account the tensile force developed in the root reinforcement and considering the same in the Mohr-Coulomb's equation in its modified form as

$$S_R = S + \Delta S = c + \sigma \tan \phi + \Delta S \quad (4.14)$$

where S_R is the shear strength of reinforced soil, S is the shear strength of unreinforced soil, ΔS is the shear strength increase caused by plant root reinforcement, σ is the total normal confining stress applied on the shear/failure plane and c and ϕ are shear strength parameters, namely, the cohesion intercept and angle of shearing resistance, respectively, of the unreinforced soil. This model is based on the observations made when the root-permeated cylindrical soil specimens of 250-mm diameter were brought to zero matric potential and sheared in a large direct shear device. The roots are assumed to be vertical, flexible, elastic, of uniform diameter and extending an equal distance on either side of the horizontal shear plane. Only the partial mobilization of fibre tensile strength is considered depending upon the amount of fibre elongation during the shear. This model does not place any constraint on the distribution or location of the reinforcing fibres.

Note that the plant roots increase the soil shear strength both directly by mechanical reinforcing and indirectly through water removal by transpiration.

4.3.2 Gray and Ohashi (GO) Model

The concept of the Waldron model was extended by Gray and Ohashi (1983) to describe the deformation and the failure mechanism of fibre-reinforced cohesionless soil and to estimate the contribution of fibre reinforcement to increasing the shear strength of soil. The model consists of a long, elastic fibre, extending an equal length over either side of a potential shear plane in sand (Fig. 4.3). The fibre may be oriented initially perpendicular to the shear plane or at some arbitrary angle i with the horizontal. Shearing causes the fibre to distort, thereby mobilizing the tensile resistance in the fibre. The tensile force in the fibre can be divided into components normal and tangential to the shear plane. The normal component increases the confining stress on the failure plane, thereby mobilizing additional shear resistance in the sand, whereas the tangential component directly resists the shear. The fibre is assumed to be thin enough that it offers little if any resistance to shear displacement from the bending stiffness. If many fibres are present, their cross-sectional areas are computed, and the total fibre concentration is expressed in terms of the *fibre area ratio*, A_r , defined by Eq. (2.7) as reproduced below:

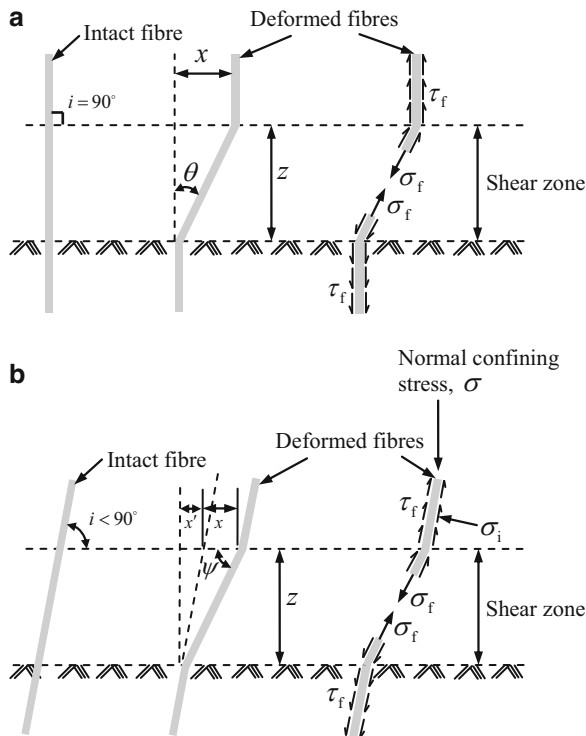
$$A_r = \frac{A_f}{A} \quad (4.15)$$

where A_f is the total cross-sectional area of fibres in a plane (e.g. shear/failure plane) within the reinforced soil mass and A is the total area of the plane (e.g. shear/failure plane) within the reinforced soil mass, which includes the soil particles, fibres and voids.

Fig. 4.3 Model for flexible, elastic fibre reinforcement, extending across the shear zone of thickness z :

(a) $i = 90^\circ$; (b) $i < 90^\circ$

(Adapted from Gray and Ohashi 1983; Shukla et al. 2009)



The shear strength increase ΔS ($=S_R - S$, S_R and S are shear strengths of reinforced soil and unreinforced soil, respectively) from the fibre reinforcement in sand can be estimated from the following expressions:

$$\Delta S = \sigma_R (\sin \theta + \cos \theta \tan \phi) \quad (4.16)$$

for fibres oriented initially perpendicular to the shear plane (Fig. 4.3a), and

$$\begin{aligned} \Delta S &= \sigma_R [\sin (90^\circ - \psi) + \cos (90^\circ - \psi) \tan \phi] \\ &= \sigma_R (\cos \psi + \sin \psi \tan \phi) \end{aligned} \quad (4.17)$$

for fibres oriented initially at some arbitrary angle i with the horizontal (Fig. 4.3b), with

$$\psi = \tan^{-1} \left(\frac{z}{x + x'} \right) = \tan^{-1} \left(\frac{1}{k + \cot i} \right) \quad (4.18)$$

where σ_R is the mobilized tensile strength of fibres per unit area of fibre-reinforced granular soil, which mainly comes from the fibres; ϕ is the angle of internal friction of unreinforced soil; θ is the angle of shear distortion; x is the horizontal shear displacement; z is the thickness of shear zone; i is the initial orientation angle of the

fibre with respect to shear surface, $x' = z \cot i$; and $k(=x/z)$ is the shear distortion ratio.

The mobilized tensile strength of fibres per unit area of soil (σ_R) can be estimated as

$$\sigma_R = A_f \sigma_f = \left(\frac{A_f}{A} \right) \sigma_f \quad (4.19)$$

where σ_f is the maximum tensile stress developed in the fibre at the shear plane, which depends upon a number of parameters and the test variables. The fibres must be long enough and frictional enough to avoid the pullout; conversely, the confining stress must be high enough so that the pullout forces do not exceed the skin friction (i.e. interface shear forces) along the fibre. It is also necessary to assume some sort of tensile stress distribution along the length of the fibre. Two likely or reasonable possibilities are linear and parabolic distributions, with tensile stress a maximum at the shear plane and decreasing to zero at the fibre ends. The resulting tensile stresses at the shear plane for these two distributions are given by the following expressions (Waldron 1977):

$$\sigma_f = \left(\frac{4E_f \tau_f}{D} \right)^{1/2} [z(\sec \theta - 1)]^{1/2} \quad (4.20)$$

for the linear distribution, and

$$\sigma_f = \left(\frac{8E_f \tau_f}{3D} \right)^{1/2} [z(\sec \theta - 1)]^{1/2} \quad (4.21)$$

for the parabolic distribution, where E_f is the modulus or longitudinal stiffness of the fibre, τ_f is the skin friction stress along the fibre and D is the diameter of fibre.

The GO model has been found to predict correctly the influence of various parameters (fibre area ratio, fibre length, fibre modulus, initial fibre orientation and sand relative density), which govern the shear strength of fibre-reinforced soil as observed in the direct shear tests conducted by Gray and Ohashi (1983). For example, in the direct shear tests, the maximum shear strength increase, both theoretically and experimentally, was observed for the fibres placed at an angle of 60° with the shear plane, that is, in the direction of major principal strain.

Note that a variation of Waldron force-equilibrium model was proposed by Jewell and Worth (1987) by placing the stiff reinforcement symmetrically, that is, extended equally about the central horizontal/shear plane in direct shear tests. The force in the reinforcement acting across the shear plane is resolved into components normal and tangential to the shear plane. These two components of the reinforcement force are considered to improve the shearing strength of the soil by directly reducing the shear force acting on the soil and by increasing the available frictional shearing resistance in the soil. The expression for shear strength increase presented

by Jewell and Worth (1987) is similar to those proposed by Waldron (1977) and Gray and Ohashi (1983) (Eqs. (4.16) and (4.17)).

4.3.3 Maher and Gray (MG) Model

Based on the observations made in triaxial compression tests and statistical analysis of strength of randomly distributed fibre-reinforced sand, Maher and Gray (1990) proposed a model for predicting its strength behaviour when subjected to static loads. The model considers the following assumptions:

1. The reinforcing fibres have a constant length and diameter, and they do not offer any resistance to bending.
2. The smaller portion of a fibre length on either side of the failure plane is uniformly distributed between zero and half of the fibre length.
3. The fibres have an equal probability of making all possible angles with any arbitrarily chosen fixed axis, that is, the failure surfaces in triaxial compression tests on granular soil are planar and oriented in the same manner as predicted by the Mohr-Coulomb failure criterion.
4. The fibres in the soil mass and, equivalently, their points of intersection with any failure plane are randomly distributed following a Poisson-type distribution.
5. For the sand-fibre composites, the principal stress envelope, that is, the plot of major principal stress at failure (σ_{1f}) versus the minor principal stress (confining stress) (σ_3), is either curved linear or bilinear, with the transition or the break occurring at a threshold confining stress, referred to as the *critical confining stress*, σ_{3crit} (Fig. 4.4). For $\sigma_3 < \sigma_{3crit}$, the fibres slip during deformation, and for $\sigma_3 > \sigma_{3crit}$, they stretch or yield. Assuming a Mohr-Coulomb failure criterion, the reinforced soil envelope is parallel to that of unreinforced soil above the critical confining stress.

The increase in shear strength from the fibre reinforcement can be estimated from the following expressions:

$$\Delta S = N_s \left(\frac{\pi D^2}{4} \right) (2a_r \sigma_{3av} \tan \delta) (\sin \theta + \cos \theta \tan \phi) \eta \quad (4.22)$$

for $0 < \sigma_{3av} < \sigma_{3crit}$, and

$$\Delta S = N_s \left(\frac{\pi D^2}{4} \right) (2a_r \sigma_{3crit} \tan \delta) (\sin \theta + \cos \theta \tan \phi) \eta \quad (4.23)$$

for $\sigma_{3av} > \sigma_{3crit}$, where σ_{3av} is average confining stress in the triaxial chamber, N_s is the average number of fibres intersecting a unit area of the shear plane, a_r is the aspect ratio of fibres, δ is the fibre skin friction angle and η is an empirical

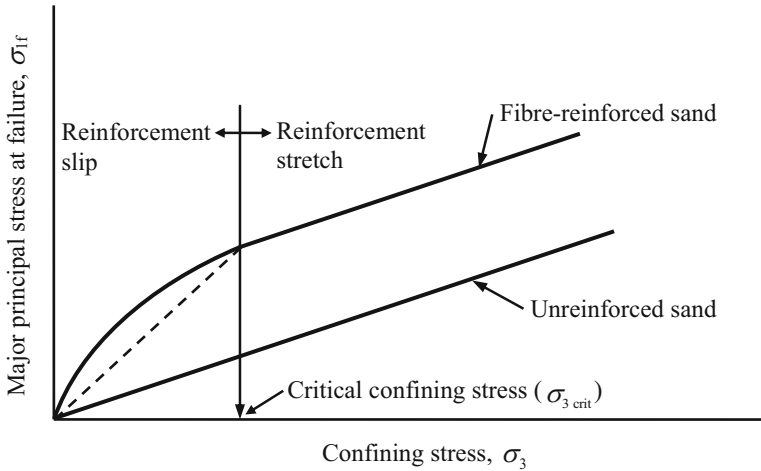


Fig. 4.4 Effect of the fibre inclusion in sand on its principal stress envelope obtained from the triaxial compression tests (Adapted from Maher and Gray 1990; Shukla and Sivakugan 2010)

coefficient depending on the soil characteristics (median/average particle size D_{50} , particle sphericity S_s and coefficient of uniformity C_U) and the fibre parameters (aspect ratio and skin friction). The value of σ_{3crit} can be determined empirically from the experimental measurements, thus depending on the soil characteristics and the fibre properties.

Note that in Fig. 4.4, for $\sigma_3 < \sigma_{3crit}$, the stress envelope for fibre-reinforced sand is either linear or nonlinear depending on the types of sand and reinforcement.

The MG model has predicted the increase in the strength of the fibre-reinforced soil reasonably well when compared to the experimental values. However, the width of shear zone z , which significantly affects the increase in strength (Shewbridge and Sitar 1989, 1990), has not been determined for the reinforced soil, as it is also not determined in the Waldron and GO models. Also, the average expected orientation of fibres is statistically predicted to be perpendicular to the plane of shear failure. It is difficult to determine experimentally the exact orientation of fibres. Note that the model proposed by Jewell and Worth (1987) for stiff reinforcements also does not pay an attention to the formation of shear zone, which significantly affects the increase in shear strength of reinforced soil.

4.3.4 Ranjan, Vasan and Charan (RVC) Model

Ranjan et al. (1996) proposed a model based on the statistical/regression analysis of the data obtained from more than 500 triaxial compression tests on the randomly distributed discrete fibre-reinforced soil. This model quantifies the effect of fibre

properties, soil characteristics and confining stress on the shear strength of the reinforced soil. The mathematical expression of the model is as follows:

$$\sigma_{1f} = f(p_f, a_r, f^*, f, \sigma_3) \quad (4.24)$$

where σ_{1f} is the major principal stress at failure of fibre-reinforced soil (i.e. shear strength of fibre-reinforced soil), p_f is the fibre content, a_r is the fibre aspect ratio, f^* is the surface friction coefficient, f is the coefficient of friction and σ_3 is the confining stress. The expressions for f and f^* are given below:

$$f = \frac{c}{\sigma} + \tan \phi \quad (4.25)$$

and

$$f^* = \frac{c_a}{\sigma} + \tan \phi_i \quad (4.26)$$

where σ is the total normal confining stress applied on the shear/failure plane; c and ϕ are shear strength parameters, namely, the cohesion intercept and angle of shearing resistance, respectively, of the unreinforced soil; c_a is the adhesion intercept; and ϕ_i is the angle of skin friction as determined from fibre pullout tests. A value of 100 kPa for σ may be adopted for calculating f and f^* using Eqs. (4.25) and (4.26), respectively. The regression analysis has considered the following assumptions:

1. The response parameter σ_{1f} is a random quantity with normal distribution law, which is followed by most distributions in nature.
2. The variance of σ_{1f} does not depend on its absolute value. That is, the variances are homogeneous.
3. The values of independent factors (i.e. $p_f, a_r, f^*, f, \sigma_3$, etc.) are not random quantities.

The failure envelope of fibre-reinforced soil is curvilinear with a transition at certain confining stress, called the critical confining stress σ_{3crit} (see Fig. 4.4).

For $\sigma_3 \leq \sigma_{3crit}$,

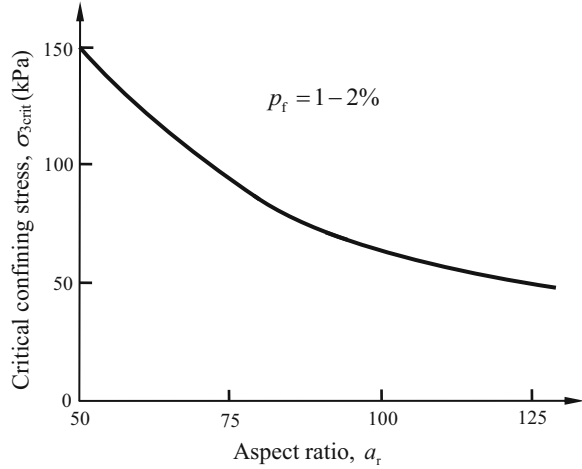
$$\sigma_{1f} = 12.3(p_f)^{0.4}(a_r)^{0.28}(f^*)^{0.27}(f)^{1.1}(\sigma_3)^{0.68} \quad (4.27)$$

For $\sigma_3 \geq \sigma_{3crit}$,

$$\sigma_{1f} = 8.78(p_f)^{0.35}(a_r)^{0.26}(f^*)^{0.06}(f)^{0.84}(\sigma_3)^{0.73} \quad (4.28)$$

Note that the values of coefficient of determination R^2 in Eqs. (4.27) and (4.28) are found to be greater than 0.90, which indicates a good fit of the data used. The value of σ_{3crit} is observed to decrease with an increase in aspect ratio a_r of fibres, as indicated in Fig. 4.5; however, it is relatively unaffected by the amount of fibre

Fig. 4.5 Effect of aspect ratio a_f on critical confining stress σ_{3crit} for plastic fibre-reinforced soil (Adapted from Ranjan et al. 1996)



content p_f as indicated in Fig. 4.5, where the data points of both $p_f = 1\%$ and $p_f = 2\%$ have been represented by the same curve.

4.3.5 Zornberg Model

Zornberg (2002) presented a discrete model for predicting the shear strength of fibre-reinforced soil based on the independent properties of fibres and soil (e.g. fibre content, fibre aspect ratio and shear strength of unreinforced soil). The fibres are assumed to contribute to the shear strength increase by mobilizing tensile stress along the plane of shear (Fig. 4.6). Therefore, the shear strength S_R of fibre-reinforced soil has the following two components: the shear strength S of soil matrix and the fibre-induced distributed tensile force per unit area σ_R . Thus

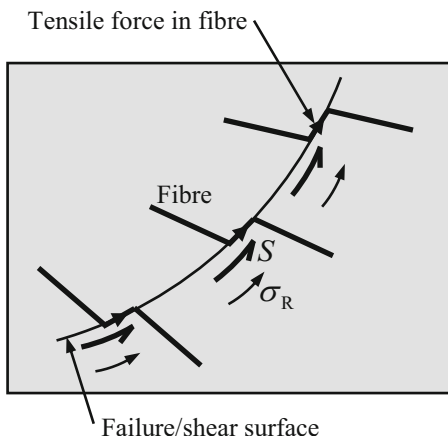
$$S_R = S + \alpha\sigma_R = c + \sigma \tan \phi + \alpha\sigma_R \tag{4.29}$$

where σ is the total normal confining stress applied on the shear/failure plane, c and ϕ are the cohesion intercept and angle of shearing of the unreinforced soil and α is an empirical coefficient that accounts for the orientation of fibres. For the case of randomly oriented fibres, α equals 1. For any preferred orientation, α should be selected suitably between 0 and 1.

Under low confining stresses, when the failure is governed by pullout of the fibres, the fibre-induced distributed tensile force can be estimated as

$$\sigma_{RP} = a_f p_{vf} (c_{i,c} c + c_{i,\phi} \sigma \tan \phi) \tag{4.30}$$

Fig. 4.6 A fibre-reinforced soil mass with fibres intersecting the failure/shear surface



where a_r is the fibre aspect ratio, p_{vf} is the volumetric fibre content and σ is the average normal stress acting on the fibres. The parameters $c_{i,c}$ and $c_{i,\phi}$ are interaction coefficients defined as

$$c_{i,c} = \frac{a}{c} \quad (4.31)$$

$$c_{i,\phi} = \frac{\tan \delta}{\tan \phi} \quad (4.32)$$

where a is the adhesion between the soil and the fibre and δ is the interface friction angle.

Note that the fibre-induced distributed tension is a function of fibre content p_{vf} , fibre aspect ratio a_r and interaction coefficients $c_{i,c}$ and $c_{i,\phi}$ if the failure is governed by the fibre pullout.

Using Eq. (4.30) with $\sigma_R = \sigma_{RP}$, Eq. (4.29) is expressed to obtain the shear strength of fibre-reinforced soil when the failure is governed by fibre pullout as

$$S_{RP} = c + \sigma \tan \phi + \alpha \sigma_R = c + \sigma \tan \phi + \alpha [a_r p_{vf} (c_{i,c} c + c_{i,\phi} \sigma \tan \phi)]$$

or

$$S_{RP} = c_{RP} + (\tan \phi)_{RP} \sigma \quad (4.33)$$

where

$$c_{RP} = (1 + \alpha a_r p_{vf} c_{i,c}) c \quad (4.34)$$

and

$$(\tan \phi)_{\text{RP}} = (1 + \alpha a_r p_{\text{vf}} c_{\text{i},\phi}) \tan \phi \quad (4.35)$$

When failure is governed by the yielding of the fibres, that is, the fibre tensile breakage, the fibre-induced distributed tensile force is a function of fibre content p_{vf} and tensile strength $\sigma_{\text{f,ult}}$ of individual fibres and can be estimated as

$$\sigma_{\text{Rt}} = p_{\text{vf}} \sigma_{\text{f,ult}} \quad (4.36)$$

Using Eq. (4.36) with $\sigma_{\text{R}} = \sigma_{\text{Rt}}$, Eq. (4.29) is expressed to obtain the shear strength of fibre-reinforced soil when the failure is governed by the tensile breakage of the fibres as

$$S_{\text{Rt}} = c_{\text{Rt}} + (\tan \phi)_{\text{Rt}} \sigma \quad (4.37)$$

where

$$c_{\text{Rt}} = c + \alpha p_{\text{vf}} \sigma_{\text{f,ult}} \quad (4.38)$$

and

$$(\tan \phi)_{\text{Rt}} = \tan \phi \quad (4.39)$$

Note that Zornberg (2002) presented the discrete model for the design of fibre-reinforced soil slopes. The fibres as discrete elements are considered to contribute to stability by mobilizing tensile stresses along the shear/failure surface, as shown in Fig. 4.6. At the critical normal stress,

$$\sigma_{\text{RP}} = \sigma_{\text{Rt}} \quad (4.40)$$

Using Eqs. (4.30) and (4.36) with $\sigma = \sigma_{\text{crit}}$, the expression for σ_{crit} is obtained as

$$\sigma_{\text{crit}} = \frac{\sigma_{\text{f,ult}} - a_r c_{\text{i},c} c}{a_r c_{\text{i},\phi} \tan \phi} \quad (4.41)$$

Thus, the critical normal stress σ_{crit} at which the governing mode of fibre failure changes from fibre pullout to fibre breakage is a function of tensile strength of fibres, soil shear strength and aspect ratio, but is independent of the fibre content.

Note that the pullout resistance of a fibre of length L , if required to be quantified, should be estimated over the shortest side of the two portions of the fibre intercepted by the failure surface. The length of the shortest portion of the fibre intercepted by the failure surface varies from zero to $L/2$. Statistically, the average embedment length of randomly distributed fibres, $L_{\text{e,av}}$, can be defined analytically as $L_{\text{e,av}} = L/4$ (Zornberg 2002).

4.3.6 Shukla, Sivakugan and Singh (SSS) Model

Shukla et al. (2010) developed a simple analytical model for predicting the shear strength behaviour of fibre-reinforced granular soils under high confining stresses, where it can be assumed that pullout of fibres does not take place. The derivation of the analytical expression is presented below.

The shear strength of the unreinforced dry granular soil is given as (Lambe and Whitman 1979; Shukla 2014)

$$S = \sigma \tan \phi \quad (4.42)$$

where σ is the total normal confining stress applied on the shear plane and ϕ is the angle of shearing resistance (or the angle of internal friction) of the granular soil.

Most of the experimental studies have shown that if fibres are added to the granular soil, there is an increase in shear strength of the soil. Assuming no pullout under high confining stresses, the increase in shear strength ΔS for the systematically distributed/oriented fibre-reinforced granular soil as shown in Fig. 4.3b can be expressed by Eq. (4.17) (Gray and Ohashi 1983).

Addition of Eqs. (4.17) and (4.42) gives the shear strength S_R of the systematically oriented fibre-reinforced granular soil as

$$S_R = S + \Delta S = \sigma_R \cos \psi + (\sigma + \sigma_R \sin \psi) \tan \phi \quad (4.43)$$

Assuming that the unreinforced granular soil does not carry any tensile stress, the mobilized tensile strength per unit area of reinforced granular soil (σ_R) can be estimated using Eq. (4.19).

Note that the fibres are assumed long enough and frictional enough to resist pullout; conversely the confining stress must be high enough to ensure that pullout forces do not exceed skin friction (i.e. interface shear forces) along the fibre. It is also necessary to assume some form of tensile stress distribution along the length of the fibre. Assuming a constant shear stress distribution along the length of the fibre, an expression for the tensile stress σ_f developed in the fibre can be derived as

$$\sigma_f \times \left(\frac{\pi D^2}{4}\right) = \left[\left(\frac{L}{2} \times \pi D\right)(\sigma_i)\right] \tan \phi_i \sin i$$

or

$$\sigma_f = 2\sigma_i \left(\frac{L}{D}\right) \tan \phi_i \sin i = 2\sigma_i a_r \tan \phi_i \sin i \quad (4.44)$$

where σ_i is normal stress on the fibre inclined to the horizontal at an angle i ; L and D are the length and the diameter of the fibres, respectively; $a_r (=L/D)$ is the aspect ratio of the fibres; and ϕ_i is the fibre-soil interface friction angle. The expression for σ_i is given as (Jewell and Wroth 1987)

$$\sigma_i = \left[\frac{1 - \sin \phi \sin (\phi - 2i)}{\cos^2 \phi} \right] \sigma \quad (4.45)$$

The term $\sin i$ is included in Eq. (4.44) as an empirical scaling constant to account for the fibre orientation. From Eq. (4.44), for $i = 0^\circ$, $\sigma_f = 0$, which indicates that if fibres are not stretched and are oriented parallel to the shear plane, they will have no tension, because shear mobilization does not take place in the absence of anchoring of the ends of fibres. Here $\sigma_i = \sigma$. For $i = 90^\circ$, $\sin i = 1$, and $\sigma_f \neq 0$. In fact, when fibres are normal to the shear plane, one can expect that the maximum shear mobilization takes place due to full anchoring of the ends of the fibres. Substituting Eq. (4.45) into Eq. (4.44) gives

$$\sigma_f = 2\sigma a_r \tan \phi_i \sin i \left[\frac{1 - \sin \phi \sin (\phi - 2i)}{\cos^2 \phi} \right] \quad (4.46)$$

Substituting Eqs. (4.19) and (4.46) into Eq. (4.43) yields

$$S_R = c_R + \sigma_{RS} \tan \phi \quad (4.47)$$

where

$$c_R = \sigma \left[2A_r a_r \tan \phi_i \sin i \cos \psi \left\{ \frac{1 - \sin \phi \sin (\phi - 2i)}{\cos^2 \phi} \right\} \right] \quad (4.48)$$

and

$$\sigma_{RS} = \sigma \left[1 + 2A_r a_r \tan \phi_i \sin i \sin \psi \left\{ \frac{1 - \sin \phi \sin (\phi - 2i)}{\cos^2 \phi} \right\} \right] \quad (4.49)$$

Comparing Eqs. (4.42) and (4.47), it can be seen that the effect of reinforcing with systematically oriented fibres is to introduce an apparent cohesion c_R to the granular soil and to increase the normal confining stress on the shear plane from σ to σ_{RS} , thereby increasing the shear strength of granular soil. The parameters c_R and σ_{RS} are the apparent cohesion and improved confining normal stress in the fibre-reinforced granular soil. Note that both c_R and σ_{RS} are functions of area ratio A_r , aspect ratio a_r , skin friction δ , normal confining stress σ and distortion angle ψ .

The shear strength improvement of the granular soil due to inclusion of fibres can be described in terms of a dimensionless ratio, called the *shear strength ratio* (*SSR*), as defined below:

$$SSR = \frac{S_R}{S} \quad (4.50)$$

Substituting Eqs. (4.42) and (4.47) into Eq.(4.50) gives

$$SSR = 1 + 2A_r a_r \left[\frac{1 - \sin \phi \sin(\phi - 2i)}{\cos^2 \phi} \right] \left(\sin \psi + \frac{\cos \psi}{\tan \phi} \right) \tan \phi_i \sin i \quad (4.51)$$

In a very thin element of the randomly distributed fibre-reinforced soil (Fig. 4.7), if $A_{f1}, A_{f2}, A_{f3}, \dots, A_{fn}$ are the areas of cross section of the fibres at a shear plane, A_{soil} is the area of the soil section, including voids at the shear plane, and ΔL is the thickness of the element measured perpendicular to the shear plane, the area ratio $A_r (=A_f/A)$ of the randomly distributed fibre-reinforced soil at the shear plane can be expressed as

$$A_r = \frac{A_f}{A} = \frac{(A_{f1} + A_{f2} + A_{f3} + \dots + A_{fn})}{(A_{f1} + A_{f2} + A_{f3} + \dots + A_{fn}) + A_{soil}} \times \frac{\Delta L}{\Delta L} = \frac{V_{sf}}{V_{sf} + V_{soil}} \quad (4.52)$$

where V_{sf} is the volume of fibre solids and V_{soil} is the volume of soil, including voids, in the element of the fibre-reinforced soil.

Eq. (4.52) can be rearranged as

$$\frac{V_{sf}}{V_{soil}} = \frac{\left(\frac{A_f}{A}\right)}{1 - \left(\frac{A_f}{A}\right)} = \frac{A_r}{1 - A_r} \quad (4.53)$$

The ratio of weight of the fibre solids W_{sf} to the weight of the soil solids W_{ss} , called the fibre content p_f , in an element of reinforced soil (Fig. 4.7), can be expressed as

$$p_f = \frac{W_{sf}}{W_{ss}} = \frac{V_{sf} G_f \gamma_w}{V_{ss} G \gamma_w} = \frac{V_{sf} G_f (1 + e_s)}{V_{soil} G} = \frac{G_f (1 + e_s)}{G_m} \left(\frac{A_r}{1 - A_r} \right) \quad (4.54)$$

or

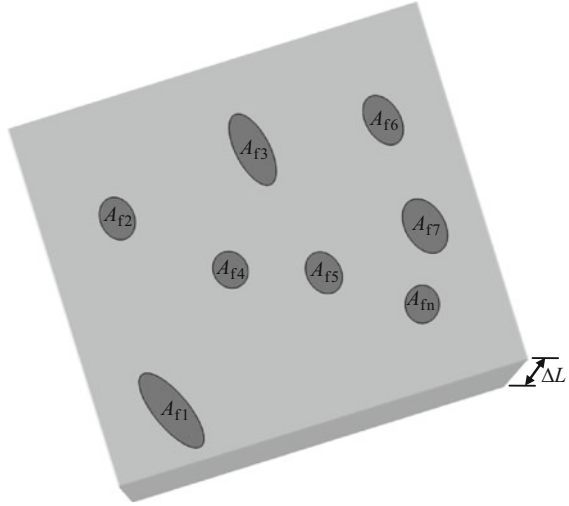
$$A_r = \frac{p_f \left[\frac{G}{G_f(1+e_s)} \right]}{1 + p_f \left[\frac{G}{G_f(1+e_s)} \right]} \quad (4.55)$$

where G_f is the specific gravity of fibre solids, G is specific gravity of soil solids and e_s is the void ratio of soil.

Substituting Eq. (4.55) into Eqs. (4.48), (4.49) and (4.51) provides

$$\frac{c_R}{\sigma} = 2a_r \tan \phi_i \sin i \cos \psi \left[\frac{p_f \left\{ \frac{G}{G_f(1+e_s)} \right\}}{1 + p_f \left\{ \frac{G}{G_f(1+e_s)} \right\}} \right] \left[\frac{1 - \sin \phi \sin(\phi - 2i)}{\cos^2 \phi} \right] \quad (4.56)$$

Fig. 4.7 An element of fibre-reinforced granular soil of thickness ΔL



$$\frac{\sigma_{RS} - \sigma}{\sigma} = 2a_r \tan \phi_i \sin i \sin \psi \left[\frac{p_f \left\{ \frac{G}{G_f(1+e_s)} \right\}}{1 + p_f \left\{ \frac{G}{G_f(1+e_s)} \right\}} \right] \left[\frac{1 - \sin \phi \sin(\phi - 2i)}{\cos^2 \phi} \right] \tag{4.57}$$

and

$$SSR = 1 + 2a_r \tan \phi_i \sin i \left(\sin \psi + \frac{\cos \psi}{\tan \phi} \right) \left[\frac{1 - \sin \phi \sin(\phi - 2i)}{\cos^2 \phi} \right] \times \left[\frac{p_f \left\{ \frac{G}{G_f(1+e_s)} \right\}}{1 + p_f \left\{ \frac{G}{G_f(1+e_s)} \right\}} \right] \tag{4.58}$$

Considering a uniform strain distribution, the stress-strain relationship for the fibre can be expressed as

$$\begin{aligned} \sigma_f &= E_f \left[\frac{\sqrt{(x+x')^2 + z^2} - \sqrt{x'^2 + z^2}}{\sqrt{x'^2 + z^2}} \right] = E_f \left(\frac{\sqrt{z^2 + z^2 \cot^2 \psi}}{\sqrt{z^2 + z^2 \cot^2 i}} - 1 \right) = \\ &= E_f \left(\frac{\sin i}{\sin \psi} - 1 \right) \end{aligned} \tag{4.59}$$

where E_f is the Young's modulus of elasticity of fibres in extension. Comparing Eq. (4.46) with Eq. (4.59) yields

$$\sin \psi = \frac{\sin i}{1 + 2a_r \tan \phi_1 \sin i \left(\frac{\sigma}{E_f} \right) \left[\frac{1 - \sin \phi \sin (\phi - 2i)}{\cos^2 \phi} \right]} \quad (4.60)$$

and

$$\cos \psi = \frac{\sqrt{\cos^2 i + 4a_r \tan \phi_1 \sin i \left(\frac{\sigma}{E_f} \right) \left[\frac{1 - \sin \phi \sin (\phi - 2i)}{\cos^2 \phi} \right] \left[1 + a_r \tan \phi_1 \sin i \left(\frac{\sigma}{E_f} \right) \left\{ \frac{1 - \sin \phi \sin (\phi - 2i)}{\cos^2 \phi} \right\} \right]}}{1 + 2a_r \tan \phi_1 \sin i \left(\frac{\sigma}{E_f} \right) \left[\frac{1 - \sin \phi \sin (\phi - 2i)}{\cos^2 \phi} \right]} \quad (4.61)$$

Substituting values of $\sin \psi$ and $\cos \psi$ from Eqs. (4.60) and (4.61), respectively, into Eq. (4.56), (4.57) and (4.58) gives the following:

$$\frac{c_R}{\sigma} = 2\beta_1 \beta_2 \left[\frac{p_f \left\{ \frac{G}{G_f(1+e_s)} \right\}}{1 + p_f \left\{ \frac{G}{G_f(1+e_s)} \right\}} \right] \left[\frac{\sqrt{\cos^2 i + 4\beta_1 \beta_2 \left(\frac{\sigma}{E_f} \right) \left[1 + \beta_1 \beta_2 \left(\frac{\sigma}{E_f} \right) \right]}}{1 + 2\beta_1 \beta_2 \left(\frac{\sigma}{E_f} \right)} \right] \quad (4.62)$$

$$\frac{\sigma_{RS} - \sigma}{\sigma} = 2\beta_1 \beta_2 \left[\frac{p_f \left\{ \frac{G}{G_f(1+e_s)} \right\}}{1 + p_f \left\{ \frac{G}{G_f(1+e_s)} \right\}} \right] \left[\frac{\sin i}{1 + 2\beta_1 \beta_2 \left(\frac{\sigma}{E_f} \right)} \right] \quad (4.63)$$

and

$$SSR = \frac{S_R}{S} = 1 + 2\beta_1 \beta_2 \left[\frac{p_f \left\{ \frac{G}{G_f(1+e_s)} \right\}}{1 + p_f \left\{ \frac{G}{G_f(1+e_s)} \right\}} \right] \times \left[\frac{\sin i}{1 + 2\beta_1 \beta_2 \left(\frac{\sigma}{E_f} \right)} + \frac{\sqrt{\cos^2 i + 4\beta_1 \beta_2 \left(\frac{\sigma}{E_f} \right) \left[1 + \beta_1 \beta_2 \left(\frac{\sigma}{E_f} \right) \right]}}{\left[1 + 2\beta_1 \beta_2 \left(\frac{\sigma}{E_f} \right) \right] \tan \phi} \right] \quad (4.64)$$

with

$$\beta_1 = a_r \tan \phi_1 \sin i \quad (4.65a)$$

and

$$\beta_2 = \frac{1 - \sin \phi \sin (\phi - 2i)}{\cos^2 \phi} \quad (4.65b)$$

Eq. (4.62) provides an expression for ratio of apparent cohesion to normal confining stress on the shear plane; Eq. (4.63) gives an expression for the ratio of increase in normal confining stress to the normal confining stress; and Eq. (4.64) defines an expression for *SSR*, which is the ratio of shear strength of reinforced soil to that of unreinforced soil.

Note that Eq. (4.64) is quite useful in predicting the variation of *SSR* with fibre content p_f , aspect ratio L/D , ratio of confining stress to modulus of fibres σ/E_f , specific gravity of fibre solids G_f and initial orientation of fibres with respect to shear plane i for any specific sets of parameters in their practical ranges. The effects of p_f , a_f and i on *SSR* for specific sets of parameters are shown in Figs. 4.8, 4.9, and 4.10, respectively.

In Fig. 4.10, you may note that as i increases, *SSR* also increases with its maximum value for $i = 74^\circ$ for the set of parameters taken. A similar trend has also been reported by Gray and Ohashi (1983) in their experimental study. They reported that an initial orientation of 60° with the shear plane is the optimum orientation for maximum increase in shear strength. This direction is approximately the principal tensile strain direction in a dense sand as reported by Jewell (1980).

For the randomly distributed fibre-reinforced soil, i can vary from 0° to 180° . For the purpose of calculating the increase in shear stress caused by inclusion of randomly distributed fibres in a granular soil, $i = 90^\circ$ can be taken for the orientation of fibres in Eq. (4.64) for simplicity in analysis. Though the observations from the analytical model matches with the experimental observations in trends of variation of parameters, it is felt that large-scale tests will be suitable for comparing the observations with the results from this model.

It is worth noting the following:

1. The inclusion of fibres in the granular soil induces cohesion, may be called the apparent cohesion, as well as an increase in the normal stress on the shear failure plane, which are proportional to the fibre content and the aspect ratio, implying that the increase in shear strength is also proportional to the fibre content and the aspect ratio.
2. The increase in shear strength of the granular soil due to presence of fibres is significantly contributed by the apparent cohesion, and the contribution to the shear strength from the increase in normal confining stress is limited.
3. As the initial orientation of fibres with respect to shear plane (i) increases, the *SSR* also increases to a maximum value for a specific value of i depending on the values of other governing parameters.

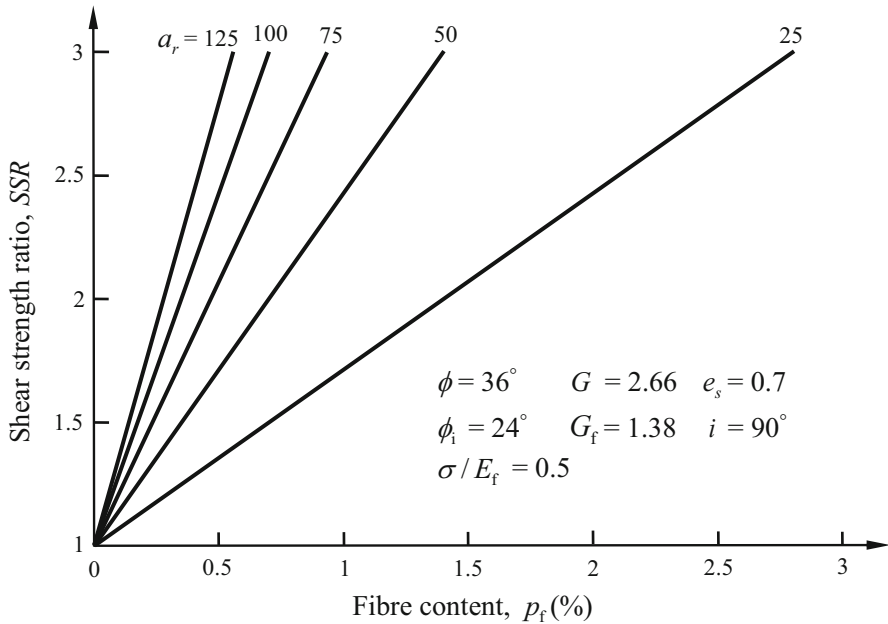


Fig. 4.8 Effect of fibre content p_f on the shear strength ratio SSR of fibre-reinforced soil (Adapted from Shukla et al. 2010)

Example 4.2

Determine the shear strength ratio (SSR) for the following three cases:

- Fibre content, $p_f = 0\%$
- Soil-fibre interface friction angle, $\delta = 0^\circ$
- All fibres are oriented parallel to the shear plane, $i = 0^\circ$

Explain the physical significance of SSR value obtained for each case.

Solution

- (a) For $p_f = 0\%$, from Eq. (4.64),

$$SSR = \frac{S_R}{S} = 1$$

This result is well expected when there are no fibres present in the soil.

- (b) For $\delta = 0^\circ$, from Eq. (2.65a), $\beta_1 = 0$, and hence from Eq. (4.64),

$$SSR = \frac{S_R}{S} = 1$$

This suggests that if fibres are not having frictional resistance in contact with soil particles, their inclusion in soil will not be useful. In this situation, there is no

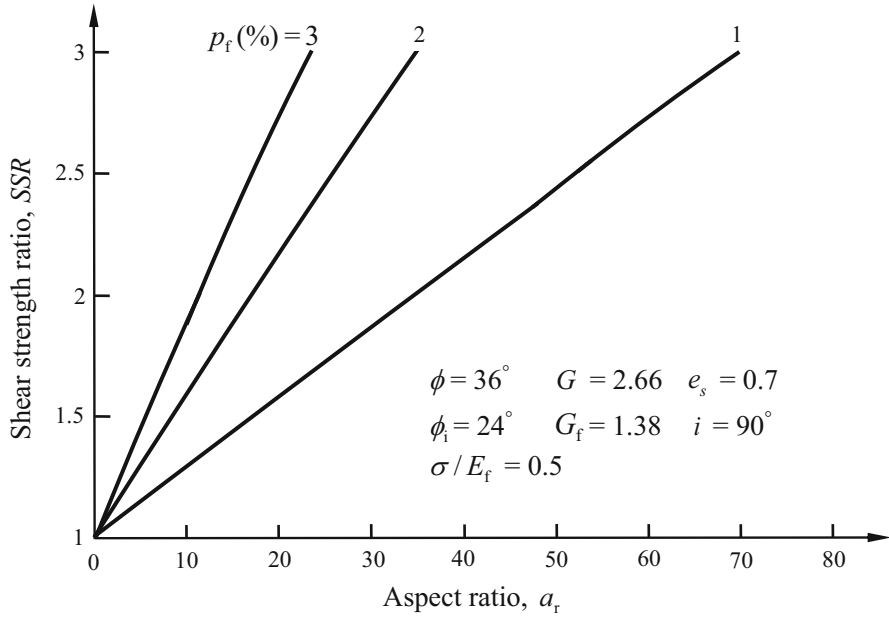


Fig. 4.9 Effect of aspect ratio a_r on the shear strength ratio SSR of fibre-reinforced soil (Adapted from Shukla et al. 2010)

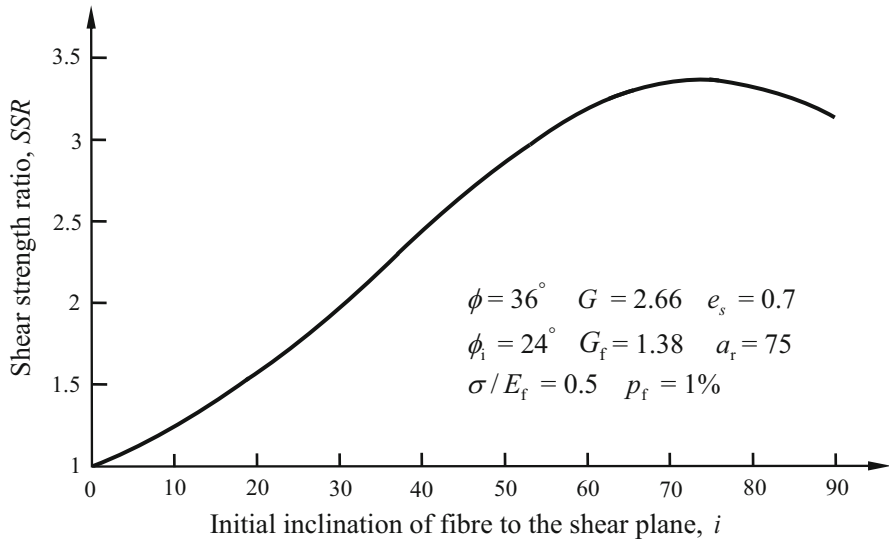


Fig. 4.10 Effect of initial inclination of fibre to the shear plane i on the shear strength ratio SSR of fibre-reinforced soil (Adapted from Shukla et al. 2010)

shear stress acting along the surface of the fibres, and therefore the fibres remain unstretched.

(c) For $i = 0^\circ$, from Eq. (2.65a), $\beta_1 = 0$, and hence from Eq. (4.64),

$$SSR = \frac{S_R}{S} = 1$$

This suggests that if all the fibres are oriented parallel to the shear plane, there will be no increase in shear strength.

4.4 Other Models and Numerical Studies

The behaviour of fibre-reinforced soils has been investigated numerically by several researchers by developing their own analysis and numerical programmes/codes or by using the commercial finite element/difference software. Some researchers have also attempted to present constitutive models based on certain assumptions for solving boundary-value problems with fibre-reinforced soils as a numerical analysis. The non-uniformity of fibre orientations and anisotropy have also been described in terms of a specific fibre orientation distribution function, resulting in an anisotropic constitutive model (Diambra et al. 2007).

Michalowski and Zhao (1996) proposed a model using the energy-based homogenization (averaging) technique to quantify the effect of fibre inclusion on the shear strength behaviour of granular soil. The model considers that the fibres contribute to the strength of the fibre-reinforced soil only if they are subjected to tension, whereas their influence in the compressive regime is neglected due to possible buckling and kinking. This model is basically a mathematical description of a failure criterion for fibre-reinforced granular soil in terms of in-plane variants q (radius of the Mohr circle representing the state of stress, that is, shear stress, $(\sigma'_1 - \sigma'_3)/2$) and p (mean of the maximum and minimum principal stresses, that is, mean principal stress, $(\sigma'_1 + \sigma'_3)/2$) in a macroscopic/global stress space as stated below:

$$\frac{q}{p_{vf}\sigma_0} = \frac{p}{p_{vf}\sigma_0} \sin \phi + \frac{1}{3}N \left[1 - \frac{1}{4a_r p_{vf}} \frac{\cot \phi_i}{\left(\frac{p}{p_{vf}\sigma_0}\right)} \right] \quad (4.66)$$

with

$$N = \frac{1}{\pi} \cos \phi + \left(\frac{1}{2} + \frac{\phi}{\pi} \right) \sin \phi \quad (4.67)$$

where p_{vf} is the volumetric fibre content, σ_0 is the yield stress of the fibre material, a_r is the aspect ratio of fibre, ϕ is the angle of internal friction of the granular matrix and ϕ_i is the soil-fibre interface friction angle.

Failure of a single fibre in a deforming fibre-reinforced soil can occur due to fibre slip or tensile rupture. When a fibre fails in the tensile rupture mode, the slip also occurs at both fibre ends up to the distance s , as given below:

$$s = \frac{D}{4} \frac{\sigma_0}{\sigma_n \tan \phi_i} \quad (4.68)$$

where σ_n is the stress normal to the fibre surface and D is the diameter of the fibre. Note that the slip also occurs at both fibre ends up to the distance s because the tensile strength of the fibre material cannot be mobilized throughout the entire fibre length. A pure slip failure mode may occur if the length of fibres L becomes less than $2s$, or when the aspect ratio

$$a_r < \frac{1}{2} \frac{\sigma_0}{\sigma_n \tan \phi_i} \quad (4.69)$$

A comparison of the Michalowski and Zhao's model with the experimental results demonstrates the adequacy of the model. When the pure slip occurs, the failure criterion takes the following form:

$$\frac{q}{p_{vf}\sigma_0} = \frac{p}{p_{vf}\sigma_0} \left(\sin \phi + \frac{1}{3} N p_{vf} a_r \tan \phi_i \right) \quad (4.70)$$

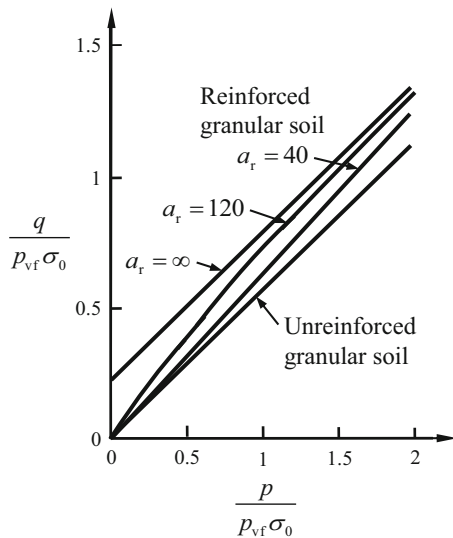
When fibres are not present, both Eqs. (4.66) and (4.70) reduce to the standard Mohr-Coulomb failure criterion for granular material as

$$q = p \sin \phi \quad (4.71)$$

Figure 4.11 shows the results from Eqs. (4.66) and (4.70) in the $q - p$ plane with different curves presenting the failure criteria for fibre-reinforced soil with fibres of various aspect ratios. As indicated in Eq. (4.70), the slip mode is described by a linear variation for a constant ϕ , whereas in the tensile rupture mode, the shear strength is not proportional to the mean stress p (Eq. (4.66)). The following points regarding Michalowski and Zhao's model are worth mentioning:

1. Five parameters (volumetric fibre concentration p_{vf} , fibre aspect ratio a_r , fibre yield stress σ_0 , internal friction angle of soil ϕ and soil-fibre interface friction angle ϕ_i) are needed to theoretically predict the failure stress. For a pure fibre slip failure mode, the failure criterion is independent of the fibre yield stress σ_0 .
2. The transition from one failure mode to another is continuous and smooth (continuous derivative).
3. The model is applicable for low value of p_{vf} , say less than 10%, so that interaction between fibres may be neglected. The length L of fibres needs to be at least one order of magnitude larger than the granular soil particle diameter, and the fibre diameter D needs to be at least of the same order as the size of granular soil particle.

Fig. 4.11 Theoretical failure criterion for fibre-reinforced granular soil (Note: $p_{vf} = 0.02$, $\phi = 35^\circ$ and $\phi_i = 20^\circ$) (Adapted from Michalowski and Zhao 1996)



4. The model is limited to isotropic mixtures, that is, the fibre-reinforced soil with isotropic distribution of fibre orientations.
5. The model indicates that the fibres may be an effective way for soil reinforcement when mixtures with a larger fibre content or larger aspect ratios are used. The stiffness of the soil prior to failure is affected by the addition of fibres, and, for flexible fibres, it drops down with respect to the stiffness of the granular soil.

The contribution of fibres to the strength of fibre-reinforced soils is very much dependent on the distribution and orientation of the fibres within the soil mass. The fibres in the direction of largest extension contribute most to the strength of the reinforced soil, whereas the fibres under compression have an adverse effect on the stiffness, and they do not produce an increase in the strength. Michalowski and Cermak (2002) presented a failure criterion for fibre-reinforced sand with an anisotropic distribution of fibre orientation, considering contribution of a single fibre to the work dissipation during failure of the reinforced sand and integrating this dissipation over all fibres in a reinforced sand element. This failure criterion can be applied directly in methods for solving stability problems for fibre-reinforced sand.

Ding and Hargrove (2006) established a nonlinear stress-strain relationship of the equivalent homogeneous and isotropic material for flexible fibre-reinforced soil, assuming there is no slip at soil-fibre interface and breakage of fibres. The development of the stress-strain relation is based on the consideration of energy in soil and energy in fibres. This constitutive model relates the shear modulus of the fibre-reinforced soil with the fibre content, distribution, geometrical features and soil-fibre interaction.

Babu et al. (2008a) presented the results of a numerical analysis of a cylindrical sand specimen (diameter = 38 mm, height = 76 mm) reinforced with the coir fibres.

They used the finite difference code, Fast Lagrangian Analysis of Continua (FLAC^{3D}), for the investigation. The results show that the presence of random fibre reinforcement in sand makes the stress concentration more diffused and restricts the shear band formation. The stress-strain response of the reinforced sand is governed by the pullout resistance of the fibres as the maximum mobilized tensile force (2.1 to 3.6 N) under different confining pressures is generally less than the tensile strength of the fibres (5 N). The mobilized tensile force in a fibre within sand increases with increasing confining pressure. No definite peak in the stress-strain diagram is observed in numerical analysis as the peaks are noticed in experimental stress-strain diagrams.

Based on the standard triaxial compression test data, Babu and Vasudevan (2008a) presented statistical models using regression for predicting the major principal stress at failure σ_{1fR} , cohesion intercept c_R , angle of internal friction ϕ_R and initial stiffness E_{iR} of soil reinforced with coir fibres, as given below:

$$\begin{aligned} \sigma_{1fR}(\text{kPa}) = & 159.1 + 3.96\sigma_3 - 0.0083\sigma_3^2 - 2959D \\ & + 4866.5D^2 - 37.01p_f + 17.35p_f^2 + 58.8L - 1.69L^2 \\ & + 2.69\sigma_3D + 548.61Dp_f + 6.21Lp_f - 0.016L\sigma_3 \end{aligned} \quad (4.72)$$

$$c_R(\text{kPa}) = 76.5 + 156.4D - 102.1D^2 + 126.1p_f - 39.3p_f^2 + 20.2Dp_f \quad (4.73)$$

$$\phi_R(\text{degrees}) = 23.1 - 78.55D + 191.1D^2 + 7.03p_f + 2.38p_f^2 - 15.02Dp_f \quad (4.74)$$

$$\begin{aligned} E_{iR}(\text{kPa}) = & 8992.2 + 64.94\sigma_3 - 0.14\sigma_3^2 - 94612D \\ & + 186594D^2 - 1744.9p_f + 1167.8p_f^2 + 1765.1L \\ & - 52.1L^2 + 33.3\sigma_3D + 11707.7Dp_f + 129.77Lp_f \\ & - 0.47L\sigma_3 \end{aligned} \quad (4.75)$$

where σ_3 is the confining pressure (kPa), D is the diameter of fibres (mm), L is the length of fibres (mm) and p_f fibre content (%). The value of R^2 for the above-presented four equations are 0.95, 0.98, 0.99 and 0.89, respectively, which are close to unity, and hence these equations can be considered satisfactory for the coir fibre-reinforced soils.

Babu and Vasudevan (2008b) have also presented regression equations for quantifying the seepage velocity and the piping resistance of coir fibre-reinforced soil considering hydraulic gradient, fibre contents and fibre lengths. In another study, Babu et al. (2008b) developed equations similar to Eqs. (4.72), (4.73) and (4.74) for coir fibre-reinforced black cotton soil and also the following expression for its compression index C_{cR} with R^2 of 0.98:

$$C_{cR} = 0.506 - 0.129p_f + 0.01p_f^2 \quad (4.76)$$

Example 4.3

A black cotton soil is reinforced with coir fibres. The fibre content is 0.2%. What is the effect of fibre inclusion on the compression index of soil?

Solution

From Eq. (4.76), the compression index of unreinforced black cotton soil ($p_f = 0\%$) is

$$C_{cU} = 0.506 - 0.129p_f + 0.01p_f^2 = 0.506 - (0.129)(0) + (0.01)(0)^2 = 0.506$$

From Eq. (4.76), the compression index of coir fibre-reinforced black cotton soil ($p_f = 0.2\%$) is

$$\begin{aligned} C_{cR} &= 0.506 - 0.129p_f + 0.01p_f^2 = 0.506 - (0.129)(0.2) + (0.01)(0.2)^2 \\ &= 0.4806 \end{aligned}$$

Thus, the compression index of black cotton soil decreases from 0.506 to 0.4806 due to inclusion of fibres. The percentage decrease is

$$\frac{\Delta C_c}{C_{cU}} \times 100 = \frac{C_{cU} - C_{cR}}{C_{cU}} \times 100 = \frac{0.506 - 0.4806}{0.506} \times 100 = \mathbf{5.02\%}$$

Diambra et al. (2010) proposed a modelling approach for coupling the effects of fibres with the stress-strain behaviour of unreinforced soil, based on the basic rule of mixtures, and presented a constitutive model for the fibre-reinforced sand mass, as stated below:

$$\Delta\sigma = \Delta\sigma' + p_{vf}\Delta\sigma_f = [M_m]\Delta\varepsilon + p_{vf}[M_f]\Delta\varepsilon \quad (4.77)$$

where $\Delta\sigma$ is the total stress increase, $\Delta\sigma'$ is the stress increase in sand particles, p_{vf} is the volumetric fibre content, $\Delta\sigma_f$ is the stress increase in fibres, M_m is the stiffness matrix for the sand, M_f is the stiffness matrix for the fibres and $\Delta\varepsilon$ is the strain increase in sand particles and fibres, caused by stress increase $\Delta\sigma$. Equation (4.77) considers that no sliding occurs between sand particles and fibres, and the fibres only act elastically in tension; thus the strains are equal in sand particles and fibres. This assumption is used in developing the stiffness matrix for the fibres. The sand stiffness matrix can be developed using the Mohr-Coulomb model or any other suitable model. In this constitutive model, any distribution of fibre orientations can be accounted for, and importance of considering the fibre orientation relative to the strain conditions can be explained. The model has been calibrated against the results of drained triaxial compression and extension tests, and a good agreement has been observed.

Note that the test results obtained from the direct shear tests conducted by Shewbridge and Sitar (1989) using a large direct shear device show that the shear zones tend to be wider in reinforced soil composites than in soil alone. The width of the shear zones increases with increasing stiffness of the composite due to any combination of increased reinforcement concentration (measured by area ratio),

stiffness and reinforcement-soil bond strength. Volume changes associated with the development of the shear zones are not spatially homogeneous. A linear relationship between reinforcement concentration and increased strength is not observed, and thus this observation contradicts the earlier observations. The actual deformation pattern of the reinforcement-soil composite can be described by a smooth asymptotic curve in the following form (Shewbridge and Sitar 1989, 1990):

$$Y = \frac{\delta}{2} (1 - e^{-k|X|}) \quad (4.78)$$

where X and Y are the axes or coordinate directions perpendicular and parallel to the direction of shear, respectively, with the origin at the centre of the shear zone (Fig. 4.12); δ is the externally applied shear displacement; and k is a deformation decay constant, which is basically a curve-fitting parameter describing the shape of the curve. The value of k can be determined from the maps of deformed soil specimens subjected to a known total shear displacement δ . The constant k provides a measure of the thickness of the shear zone and of the distribution and magnitude of shear strains within it. For the specimens with relatively thin shear zones, which contain large shear strains, the value of k is large. For the specimens with large shear zones containing small shear strains, the value of k is small. The value of k decreases as the fibre area ratio increases, that is, the shear zone width increases with an increase in reinforcement concentration. The value of k also decreases with an increase in reinforcement stiffness and soil-reinforcement interface bond strength. Thus, the shear zone width, as measured by the deformation decay constant k , increases with increasing reinforcement concentration, reinforcement stiffness and soil-reinforcement bond strength.

The deformation pattern, defined by Eq. (4.78), differs significantly from the simple shear deformation pattern assumed in the models, described in Sec. 4.3. In fact, there is still a need of further study based on large-scale field tests to investigate more realistic picture of shear zone development and width of shear zone in the fibre-reinforced soil because the shear zone significantly governs the strength and deformation of the reinforced soil.

Chapter Summary

1. If the failure occurs by rupture of the reinforcement, the strength increase can be characterized by a constant cohesion intercept c_R as an apparent cohesion, introduced due to reinforcement. If the failure occurs by a slippage between the reinforcement and the soil, the strength increase can be characterized by an increased friction angle ϕ_R . In general, a fibre-reinforced soil typically shows the bilinear strength behaviour.
2. If the failure is characterized by pullout of individual fibres, the fibre-induced distributed tension increases linearly with fibre content and fibre aspect ratio.
3. Simplified models of fibre-reinforced soil are based on different approaches, such as force-equilibrium/mechanistic approach, energy dissipation approach, statistical approach and the approach of superposition of the effects of soil and fibres.

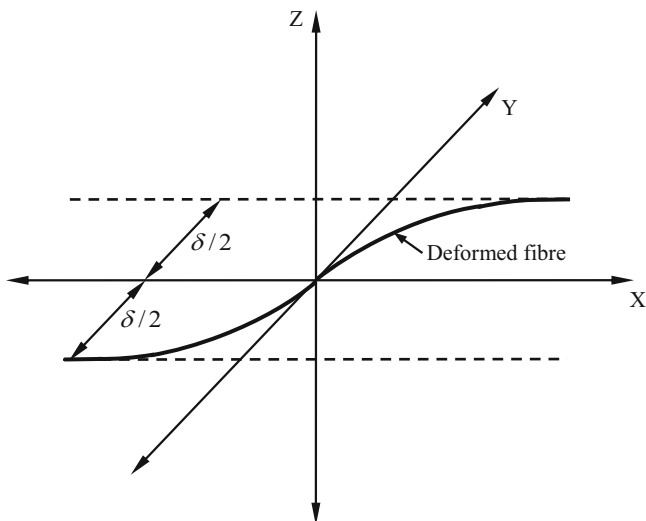


Fig. 4.12 Schematic geometry of deformed reinforcement in the coordinate space (Adapted from Shewbridge and Sitar 1989, 1990)

4. Waldron model and Gray and Ohashi (GO) model have correctly described the characteristics of reinforced soil in direct shear, in which the failure/shear plane is predetermined and the reinforcement is placed at certain angle with the failure plane. Hence these models are applicable only for oriented inclusions.
5. Maher and Gray (MG) model; Shukla, Sivakugan and Singh (SSS) model; and statistical models predict reasonably well the increase in strength of randomly distributed fibre-reinforced soils as these models are based on the triaxial compression tests.
6. The SSS model provides a more generalized analytical expression for estimating the shear strength increase as a result of fibre inclusion within the soil mass.
7. Width of shear zone should be considered for developing the models for more realistic estimation of improvement in the strength of fibre-reinforced soils.
8. Available statistical models provide the empirical expressions based on limited characteristics of soils and fibres, and hence they should not be used as the generalized expressions for estimating the engineering properties of fibre-reinforced soils.
9. Constitutive models can be developed using the basic rule of mixtures as required for any specific application. Equation (4.77) is an example of such a model, which considers that no sliding occurs between sand particles and fibres, and the fibres only act elastically in tension; thus the strains are equal in sand particles and fibres.
10. Behaviour of fibre-reinforced can be investigated numerically considering the appropriate constitutive models. Non-uniformity of fibre orientations and anisotropy can easily be considered in numerical models.

Questions for Practice

(Select the most appropriate answer to the multiple-choice questions from Q 4.1 to Q 4.5.)

- 4.1. A fibre within a soil mass can apply confining stress by
- (a) Skin friction
 - (b) Adhesion
 - (c) Both (a) and (b)
 - (d) Cohesion
- 4.2. Which of the following conditions may cause the fibres to slip during deformation of the fibre-reinforced soil?
- (a) $\sigma_3 < \sigma_{3crit}$
 - (b) $\sigma_3 > \sigma_{3crit}$
 - (c) $\sigma_3 \geq \sigma_{3crit}$
 - (d) None of the above
- 4.3. The effect of width of shear zone is not considered in
- (a) Waldron model
 - (b) GO model
 - (c) MG model
 - (d) all of the above
- 4.4. Which of the following models is a statistical/regression model?
- (a) Waldron model
 - (b) RVC model
 - (c) SSS model
 - (d) None of the above
- 4.5. Shear strength of the fibre-reinforced soil increases with
- (a) Increasing fibre content and decreasing aspect ratio
 - (b) Decreasing fibre content and increasing aspect ratio
 - (c) Increasing both fibre content and aspect ratio
 - (d) Decreasing both fibre content and aspect ratio
- 4.6. Explain the basic reinforcing mechanism of fibre-reinforced soil.
- 4.7. What is critical confining stress? Explain its importance. Derive an expression for the critical confining stress.
- 4.8. Under what conditions, the fibre reinforcement within the soil mass may slip or rupture?
- 4.9. For a reinforced sand, consider the following:
- Angle of shearing resistance of unreinforced sand, $\phi = 30^\circ$
Friction factor, $F = 0.15$
Determine the angle of shearing resistance of the reinforced sand.

- 4.10. What are the assumptions of Maher and Gray model? Is this model of fibre-reinforced soils based on observations made in triaxial compression tests? Is this model applicable to all types of fibre-reinforced soils? Justify your answer.
- 4.11. What are the limitations of GO, MO and SSS models?
- 4.12. Can you use the available statistical models as the generalized models to estimate the engineering properties of soils? Explain briefly.
- 4.13. List the parameters/factors considered in the SSS model. Derive the analytical expression for the shear strength ratio proposed by the SSS model of the fibre-reinforced soil.
- 4.14. What is the key advantage of using the Zornberg model?
- 4.15. Explain the effect of aspect ratio on the critical confining stress.
- 4.16. Using the SSS model, discuss the effects of the following on the shear strength of fibre-reinforced soil:
- Soil-fibre interface friction angle (δ)
 - Modulus of elasticity of fibres (E_f)
 - Angle of shearing resistance of soil (ϕ)
- 4.17. What is physical meaning of having the shear strength ratio (SSR) of unity for a fibre-reinforced soil?
- 4.18. Derive the following relationship:

$$SSR = 1 + \left(\frac{c_R}{\sigma}\right) \frac{1}{\tan \phi} + \frac{\sigma_{RS} - \sigma}{\sigma}$$

Show the variation of SSR , c_R/σ and $(\sigma_{RS} - \sigma)/\sigma$ with the fibre content p_f for typical values of soil and fibre parameters.

- 4.19. Explain the model of fibre-reinforced soil developed using the energy-based homogenization technique. What are the key features of this model?
- 4.20. Explain the constitutive model for the fibre-reinforced soil mass developed using the basic rule of mixtures. Is there any limitation of this model?
- 4.21. A black cotton soil is reinforced with coir fibres. The fibre content is 0.6%. What is the effect of fibre inclusion on the compression index of soil?
- 4.22. Shear zones tend to be wider in fibre-reinforced soils than in soil alone. Is it true? Justify your answer.

Answers to Selected Questions

- 4.1 (c)
 4.2 (a)
 4.3 (d)
 4.4 (b)
 4.5 (c)
 4.9 43.7°
 4.21 14.58% decrease

References

- Babu GLS, Vasudevan AK (2008a) Strength and stiffness response of coir fibre-reinforced tropical soil. *J Mat Civil Eng ASCE* 20(9):571–577
- Babu GLS, Vasudevan AK (2008b) Seepage velocity and piping resistance of coir fibre mixed soils. *J Irrig Drainage Eng ASCE* 134(4):485–492
- Babu GLS, Vasudevan AK, Haldar S (2008a) Numerical simulation of fibre-reinforced sand behaviour. *Geotext Geomembr* 26(2):181–188
- Babu GLS, Vasudevan AK, Sayida MK (2008b) Use of coir fibres for improving the engineering properties of expansive soils. *J Nat Fibers* 5(1):61–75
- Bassett RH, Last NC (1978) Reinforcing earth below footings and embankments. In: *Proceedings of symposium on earth reinforcement*, ASCE, Pittsburgh, pp 202–231
- Diambra A, Russell AR, Ibraim E, Wood DM (2007) Determination of fibre orientation distribution in reinforced sands. *Geotechnique* 57(7):623–628
- Diambra A, Ibraim E, Wood DM, Russell AR (2010) Fibre reinforced sands: experiments and modelling. *Geotext Geomembr* 28(3):238–250
- Ding D, Hargrov SK (2006) Nonlinear stress-strain relationship of soil reinforced with flexible geofibres. *J Geotech Geoenviron Eng ASCE* 132(6):791–794
- Gray DH, Al-Refeai T (1986) Behaviour of fabric versus fiber reinforced sand. *J Geotech Eng ASCE* 112(8):804–820
- Gray DH, Ohashi H (1983) Mechanics of fibre reinforcement in sand. *J Geotech Eng ASCE* 109(3):335–353
- Hausmann MR, Vagneron J (1977) Analysis of soil-fabric interaction. In: *Proceedings of international conference on the use of fabrics in geotechnics*, Paris, pp 139–144
- Jewell RA (1980) Some effects of reinforcement on the mechanical behaviour of soils. Ph.D. thesis, University of Cambridge, UK
- Jewell RA, Wroth CP (1987) Direct shear tests on reinforced sand. *Geotechnique* 37(1):53–68
- Lambe TW, Whitman RV (1979) *Soil mechanics*. SI Version. Wiley, New York
- Long NT, Guegan Y, Legeay G (1972) *Etude de la terre armee a l'appareil triaxial*. Rapport de Recherche No. 17. Laboratoire Central des Ponts et Chaussees, Paris, France
- Maher MH, Gray DH (1990) Static response of sands reinforced with randomly distributed fibres. *J Geotech Eng ASCE* 116(11):1661–1677
- Michalowski RL, Zhao A (1996) Failure of fiber-reinforced granular soils. *J Geotech Eng ASCE* 122(3):226–234
- Michalowski RL, Cermak J (2002) Strength anisotropy of fiber-reinforced sand. *Comput Geotech* 29(4):279–299
- Ranjan G, Vasan RM, Charan HD (1996) Probabilistic analysis of randomly distributed fibre-reinforced soil. *J Geotech Eng ASCE* 122(6):419–426
- Schlösser F, Vidal H (1969) Reinforced earth. *Bulletin de Liaison des Laboratoires des Ponts et Chaussees*, 41, France
- Schlösser F, Long N-T (1974) Recent results in French research on reinforced earth. *J Constr Div ASCE* 100(3):223–237
- Shewbridge SE, Sitar N (1989) Deformation characteristics of reinforced sand in direct shear. *J Geotech Eng ASCE* 115(8):1134–1147
- Shewbridge SE, Sitar N (1990) Deformation based model for reinforced sand. *J Geotech Eng ASCE* 116(7):1153–1170
- Shukla SK (2002) *Geosynthetics and their Applications*. Thomas Telford, London
- Shukla SK (2012) *Handbook of geosynthetic engineering*, 2 edn. ICE Publishing, London
- Shukla SK (2014) *Core principles of soil mechanics*. ICE Publishing, London
- Shukla SK (2016) *An introduction to geosynthetic engineering*. CRC Press/Taylor and Francis, London
- Shukla SK, Sivakugan N (2010). Discussion of “Fiber-reinforced fly ash subbases in rural roads” by P. Kumar and S.P. Singh”. *J Transp Eng ASCE* 136(4):400–401

- Shukla SK, Yin J-H (2006) Fundamentals of geosynthetic engineering. Taylor & Francis, London
- Shukla, S.K., Sivakugan, N. and Das, B.M. (2009). Fundamental concepts of soil reinforcement – an overview. *Int J Geotech Eng* 3(3):329–343
- Shukla SK, Sivakugan N, Singh AK (2010) Analytical model for fiber-reinforced granular soils under high confining stresses. *J Mat Civil Eng ASCE* 22(9):935–942
- Waldron LJ (1977) The shear resistance of root-permeated homogeneous and stratified soil. *Proc Soil Sci Soc Am* 41(5):843–849
- Yang Z (1972) Strength and deformation characteristics of reinforced sand. Ph.D. thesis, University of California, Los Angeles
- Zornberg JG (2002) Discrete framework for limit equilibrium analysis of fibre-reinforced soil. *Geotechnique* 52(8):593–604